Automatic data extraction from radargrams

Aleksandar Ristic, Aleksandra Radulovic, Miro Govedarica, Milan Vrtunski
University of Novi Sad, Faculty of Technical Sciences, Department of automation, geomatics and control systems
Trg Dositeja Obradovica 6, 21000, Novi Sad, Serbia

***Abstract*— Radargrams are result of acquisition with GPR scanning technology. Most of underground utilities has cylindrical shape and is represented in radargrams by hyperbolic signatures. In this paper a new automated procedure for hyperbolic signatures detection and data extraction in radargrams is proposed. Extracted data is the set of points which represents vectorized form of hyperbolic reflections. Resulting data from automated procedure were later used to simultaneously estimate the radius of a cylindrical object and the wave propagation velocity based on fitted hyperbola geometries. Estimation of geometry parameters and wave propagation velocity from extracted set of points is a complete solution for underground utility and soil characterization. A number of experiments showed that the procedure is robust to various types of influences.**

I. INTRODUCTION

In recent period, GPR technology has become more accessible and more present in engineering applications. This led to an increased amount of data being collected with GPR [3]. In addition, interpretation of results from the radargram (e.g., underground utility detection) is a complex task in terms of operators' knowledge and skills. Therefore, the increased amount of data and complex interpretation are pre-conditions for the development of automated procedures for detection and interpretation of anomalies in radargrams.

From a technical point of view, software detection of anomalies (hyperbolic reflections, for instance) in radargram is difficult because:

- Various types of media surrounding the objects produces excessive data (caused by different geological environments and change of volumetric moisture content)
- Incomplete or noisy hyperbolic reflections (caused by conditions of acquisition and/or media inhomogeneities)
- Interference of neighboring hyperbolic reflections (estimation of affiliation)

Procedures for radargram examination for the needs of automated detection can be performed by either analyzing the full, dense radargram image or by analyzing a thresholded sparse version of it [2]. It is possible to apply unsupervised procedures (Hough transform, for instance) and supervised procedures (e.g., Artificial Neural Networks – ANN) if dense radargram is analyzed. According to the authors' best knowledge, all existing strategies for hyperbolic reflections detection involve application of algorithms that implement Hough transform [4], Wavelet transform [5], Radon transformation [6], standard algorithms for pattern recognition, such as Support Vector Machines (SVM) [7], or ANN [8]. ANNs are easiest to train after radargram simplification has been done by edge detection [9] or binarization [10]. ANNs can trained using signal processing statistical data descriptors [11], Welch power spectral density estimate of signal segments [12] or generated data sets which model EM waves propagation in specific conditions [13], [14].

The analysis of the papers related to these technologies yields the conclusion that the search through the dense radargram is very demanding in terms of time and computation resources and sensitive to noise and hyperbolic segments interference as well. Furthermore, it can be noticed that the majority of the procedures is directed towards the analysis of simplified radargram, which can be done in two ways [3]:

1. Simplification of dense radargram and extraction of the data from the hyperbolic reflection
2. Segregation of small two-dimensional sections from dense radargram (called segment of interest - SOI) and extraction of the data from the hyperbolic reflection

The procedure presented in this paper is based on the application of the procedure with segregation of segments of interests (SOI) from dense radargram. Such procedure retains maximum possible data resolution from the radargram in one or more segregated SOIs. When the data is extracted from SOI it is possible to apply each of aforementioned techniques for data extraction regardless of their complexity, because the amount of data is significantly reduced. The proposed procedure mostly resolves problems of automated hyperbolic reflections detection. When dense radargram is reduced to one or several SOIs, the amount of data is significantly decreased but data in each zone are unchanged.

When hyperbolic reflections are incomplete and noisy, there is a significant possibility of a complete or large loss of data during the simplification of dense radargram.

II. PROCEDURE DESCRIPTION

The proposed procedure is done in three steps.

Step 1: basic pre-processing of radargram in terms of time-zero offset and *.dzt to *.bmp conversion. Software tools provide functions for this conversion, both free software (e.g. "MatGPR" [21], or "Rad2bmp" [22]) and commercial software (e.g. "RADAN" [23]).

Step 2: detection of SOI in dense radargram using ANN, that is Cascade Object Detector trained on previously formed sets of samples which contain hyperbolic reflections (positive targets) and ones that do not contain hyperbolic reflections (negative targets).

Step 3: hyperbolic reflections segregation and data extraction (x,t) in the zone of interest using an edge detection technique.

With this input data set, estimation procedures are applied. Geometric and other characteristics of manmade objects are estimated, as well as EM wave's propagation velocity, which is described in subsection B.

1) Hyperbolic reflections detection (Step 2)

Cascade Object Detector (COD) is well known algorithm for machine learning. It is based on Viola-Jones learning algorithm [15]. First, the classifier has to learn to identify an object. It is done by training during which many positive (containing object - hyperbolic reflection) and negative (not containing object - without hyperbolic reflection) sample images are analyzed (Fig. 1). After the training has been completed the output classifier can be used for object recognition. In the process of detection, the algorithm divides the input images into many sub-images by moving a search window at multiple scales over it. The each sub-window is classified as object or no-object [16].

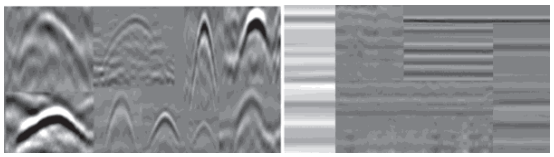

Figure 1. Example of positive (left) and negative (right) training samples

COD consists of stages with each phase representing a set of weak classifiers (Fig. 2). Weak ones are simple classifiers called 'part of decision'. Each stage is trained using the technique called 'boosting'. 'Boosting' provides the possibility to train highly precise classifier taking weighted average of decisions which are made using weak classifiers [16]. Each stage of the classifier marks a region defined by current location of the moving window as either positive or negative. Positive mark indicates that the object is found while negative mark indicates that there is no object of interest. If the mark is negative, classification in that region is over and detector moves the window to a next location. If the mark is positive, the classifier sends possibly positive region to next stage. Finally, a detector reports found object on the current location of the window, if the region is classified as positive in the final stage. Stages are designed to reject negative sample images as fast as possible. Presumption is that most of the windows do not contain object of interest. On the other hand, true positive objects are rare and it is worth to spend time for inspection of every single object. An object becomes true positive when positive sample image is correctly classified and false positive when negative sample image is misclassified as positive. An object becomes false negative when positive sample image is misclassified as negative. In order for algorithm to work correctly, each stage in the cascade must have low rate of false negative objects. If the object in the stage is mismarked as negative, classification is cancelled and it is not possible to correct the error. Moreover, each stage needs to have a high rate of false positive objects. Even if a classifier mismarks negative object as positive, the error can be corrected in next stages. Overall rate of false positive objects in cascade classifier is f^s, where f is the rate of false positives per stage in the range (0, 1) and s is the number of stages. Similarly, the overall rate of true positives is t^s, where t is the rate of true positives in the range (0, 1]. Hence, it can be noticed that adding of stages reduces overall false positives rate, but it reduces overall true positives rate as well [16].

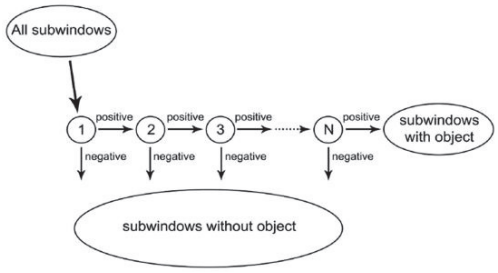

Figure 2. Schematic depiction of the detection cascade with N stages.

COD algorithm supports three training models:

- Haar-like features [16]
- LBP – Local Binary Patterns [17]
- HOG – Histograms of Oriented Gradients [18]

Each of these models has its advantages and disadvantages, so experimental evaluation of their applicability has been done, under the same conditions. The training set was comprised of more than 100 positive and more than 200 negative sample images. All used pieces of data are real (not generated) and collected in real conditions (urban and suburban area), not on test-fields (which have strictly defined parameters and acquisition conditions). The radargrams are collected using 200, 400 and 900MHz antennas, with several variations in terms of type of soil, homogeneity and volumetric moisture content.

Fig. 3 represents comparative analysis of the results of the mentioned models application. In the Fig. 3, the radargram is shown as *.bmp with time-zero offset removed. The radargram is formed on a soil with low volumetric moisture content with two pipes of large diameter (500 and 350mm) in it.

The key parameters of the experiment were training speed and accuracy (number of 'false' targets). Results yielded following conclusions:

1. Haar-like features – longest training, medium number of 'false' targets that are always present, which indicates higher sensitivity to interference.
2. LBP – shortest training, highest number of identified 'false' targets that are always present which indicates higher sensitivity to interference.
3. HOG – medium time for training, lowest number of 'false' targets identified, in most cases none.

Fig. 3a (Haar model) shows that in represented example 3 'false' objects are registered, while the time for training was 238 seconds. Fig. 3b (LBP) shows that, in represented example, 6 'false' objects are registered,

while the time for training was 7 seconds. Finally, Fig. 3c (HOG) shows that not a single 'false' object was registered in this example, while the time for training was 52 seconds.

Number of detector stages has to be defined relative to a rate of 'false' positive targets per stage: lower rate yields smaller number of stages, and vice versa. Generaly, it is better to have bigger number of simple stages with since the rate of 'false' positive targets decreases exponentionaly. Number of COD stages that produced best results in experiments was around 20.

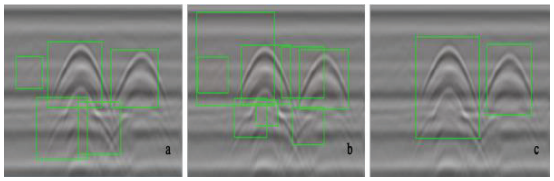

Figure 3. Results of COD algorithm trained on three data set models.

Processing of the single radargram lasts from one to several seconds depending on the length and complexity of radargram and computers processing power.

2) Hyperbolic reflections segregation and data extraction (Step 3)

Edge detection is an image processing technique, designed to recognize the edges of the object within the image [19]. Function processes a grayscale image and returns binary image with the same dimensions as the grayscale source. Binary image has 'ones' where the edge of the object is found and 'zeroes' elsewhere. Edges match significant local changes of the intensity in the image. Edge is a set of connected pixels that are on the borderline between two regions. Intensity changes are caused by different physical changes, including color, texture, reflection and shadows. Edge detection on noisy images is very difficult, since both the noise and the edges contain high-frequency components; moreover not every edge contains gradual changes of intensity [5].

Edge detection is done using "canny" operator that finds the edges by local maximum of image (radargram) gradient, which is calculated using Gauss filter [19]. The method uses two threshold values in order to detect strong and weak edges, and includes weak edges into output result only if they are connected with strong edges. The probability that the function with canny parameter will be misguided by the noise is lower, while the probability that true weak edges will be detected is higher. Application of functions for edge detection results in smaller amount of data that needs to be processed and makes this system functional in real time [12].

The result of edge detection function is boundary area (Fig. 4a). Overlapping of boundary area with the SOI, all the pixels within boundary area are multiplied by 1, while pixels outside the boundary area are multiplied by 0. That extracts only pixels within boundary area that belong to hyperbolic reflection only. Fig. 4b represents detection of maximum of pixel intensity along columns in order to ensure that only strongest reflection is saved.

These are the maximums that appear for the first time, i.e. if in one column the same maximum appears several times, the first one is taken into account.

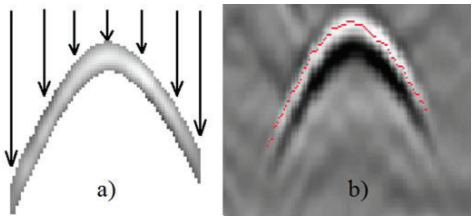

Figure 4. Hyperbolic reflection data segregation a) and finding maximum values in columns b).

3) Method to simultaneously estimate the radius of a cylindrical object (R) and the wave propagation velocity (v) - short review

Results produced by automated hyperbolic reflections procedure are used to estimate radius of a cylindrical object and the wave propagation velocity simultaneously. Considering these procedures together, they form a complete solution for automated detection of cylindrical underground objects and estimation of their parameters. Our estimation method is not the main focus of this paper so it is given here in a short review. Further details can be found in [1].

Equation (1) defines non-linear estimation model with 4 variables: x_0, t_0, R and v where (x_0, t_0) are the apex coordinates of the hyperbola optimally fitted through raw data [1].

$$\frac{\left(t+\frac{2\cdot R}{v}\right)^2}{\left(t_0+\frac{2\cdot R}{v}\right)^2}-\frac{(x-x_0)^2}{\left(\frac{v}{2}\cdot t_0+R\right)^2}=1 \qquad (1)$$

(x, t) – extracted point coordinates.

Step 1: (x_0, t_0) is estimated using a modified Levenberg–Marquardt method. The applied algorithm is robust and was adapted to solve nonlinear problems using the least squares method. The basic task of the first step is to decrease the number of correlations between the estimated parameters, i.e., to reduce the problem dimensionality from four to two correlated parameters. The estimated values (x_0, t_0) are the input data for the next step.

Step 2: estimation of boundary speed v_0. Since v is unknown (or approximately known, which is insufficient to accurately estimate R), an additional condition to simultaneously estimate v and R is defined as the velocity range [v_{max}–v_{min}]. The boundary velocity is estimated iteratively by varying v. The value closest to satisfying the condition $R\approx 0$ is accepted as v_0. A propagation velocity higher than v_0 does not make sense, because it produces negative values of R. With values known from the previous step nonlinear model (1) enables determination of unique estimation of v_0.

Step 3: simultaneous estimation of v and R. Since v is varied in the interval $[v_{max}–v_{min}]$ forming a criterion to choose v enables the selection of optimally estimated v from the set of possible values. For the selection criterion the *foo (First Order Optimality Criterion)* is chosen.

III. Experimental Results

Verification of the method was done on a number of radargrams (more than 100 typical cases). All of them contain real field data and geometry of underground objects is known (ground truth data!). Two typical radargrams are selected for discussion in this paper. The first one has low noise ratio and interference, while the other represents the opposite case.

The radargram, 6.82m long, shown in Fig. 5, is formed using 400MHz antenna, with 1 scan/cm horizontal and 512smp/scan vertical resolution. Corresponding bitmap has dimensions of 682x512 pixels. Detection of two hyperbolic reflections is correct. 203 points are extracted for the detected hyperbola on the left side (500mm diameter pipe), while 166 points are extracted for the hyperbola on the right side (350mm diameter pipe). This example contains several hyperbolic reflections (two) which are relatively close, and to a certain degree interfere with each other.

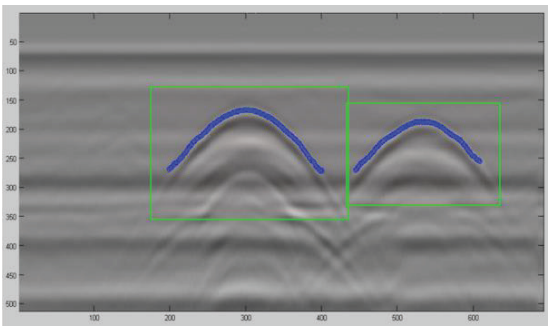

Figure 5. Original radargram and result of detection.

The radargram in Fig. 6 is 461 scan long. Five underground tanks were scanned, with vertical resolution of 512 smp/scan. Since tanks are of larger dimensions and adjacent, the interference between hyperbolic reflections is evident (marked with arrows on Fig. 6). The interference resulted with ‘false’ hyperbolic reflections. Five ‘true’ hyperbolic reflections were detected along with one ‘false’.

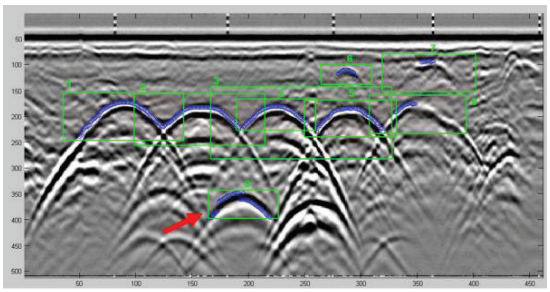

Figure 6. Original radargram and result of detection.

Detection of hyperbolic reflections proved itself as very robust to noise and incomplete hyperbolas, while not that robust to interference (it has to be emphasized that interference is not that common in real application). Edge detection also proved to be very robust, but radargrams with low signal intensity sometimes posed a problem. In some cases applying a gain to a certain degree enabled edge detection.

IV. Conclusion

In this paper, new procedure for automated detection of hyperbolic reflections and data extraction from radargrams was proposed. Procedure was tested on a number examples containing real field data and some of experimental results were shown in this paper. Experiments showed that the procedure is robust to various types of media surrounding the objects, incomplete or noisy hyperbolic reflections and that it produces satisfactory results for the needs of underground utility detection. Robustness to interference of neighboring hyperbolic reflections can be improved by adding expert knowledge to the procedure. Along with our existing parameter estimation method it represents the complete solution for underground utility characterization.

Acknowledgment

Some results represented in this paper are obtained through the project "Modeling the state and the structure of slope processes, using GNSS, TLS and GPR", founded by Ministry of science and education, project number TR 37017.

References

[1] Ristic, D. Petrovacki and M. Govedarica, “A New Method to Simultaneously Estimate the Radius of a Cylindrical Object and the Wave Propagation Velocity from GPR Data,” *Computers & Geosciences*, vol. *35*, pp. *1620-1630*, Aug., 2009.

[2] R. Janning, A. Busche, T. Horváth and L. Schmidt-Thieme, “Buried pipe localization using an iterative geometric clustering on GPR data”, *Artificial Intelligence Review*, vol. *42*, no. *3*, pp. *403-425*, Oct., 2014.

[3] S. Birkenfeld, "Automatic detection of reflexion hyperbolas in GPR data with neural networks", *in Proc. World Automation Congress (WAC 2010)*, Sept. 2010, Kobe, Japan, pp. *1189-1194*.

[4] G. Borgioli, L. Capineri, P. Falorni, S. Matucci, C. Windsor, 2008. “The detection of buried pipes from time-of-flight radar data,” *IEEE Trans. Geosci. Remote Sens.*, vol. *46*, no. *8*, pp. *2254–2266*, Aug., 2008.

[5] H. Zhou, M. Tian, X. Chen, “Feature extraction and classification of echo signal of ground penetrating radar,” *Wuhan University Journal of Natural Sciences*, vol. *10*, no. *6*, pp. *1009-1012*, Nov., 2005.

[6] A. Dell’Acqua, A. Sarti, S. Tubaro, L. Zanzi, “Detection of linear objects in GPR data”, *Signal Processing,* vol. *84*, no. *4*, pp. *785-799*, Apr., 2004.

[7] E. Passoli, F. Melgani, F. Donelli, "Automatic Analysis of GPR Images: A Pattern-Recognition Approach," *IEEE Trans. Geosci. Remote Sens.*, vol. *47*, no. *7*, pp. *2206–2217*, July, 2009.

[8] H. S. Youn, C. C. Chen, “Automatic GPR target detection and clutter reduction using neural network,” *in Proc SPIE 4758, 9th International Conference on Ground Penetrating Radar*, S. Barbara, 2002.

[9] M. R. Shaw, S. G. Millard, T. C. K. Molyneaux, M. J. Taylor, J. H. Bungey, “Location of steel reinforcement in concrete using ground penetrating radar and neural networks,” *NDT & E International,* vol. *38*, no. *3*, pp. *203-212*, Apr., 2005.

[10] P. Gamba, S. Lossani, “Neural detection of pipe signatures in ground penetrating radar images,” *IEEE Trans. Geosci. Remote Sens.,* vol. *38*, no. *2*, pp. *790-797*, Mar., 2000.

[11] S. Shihab, W. Al-Nuaimy, Y. Huang, A. Eriksen, “Neural network target identifier based on statistical features of GPR signals,” *in Proc SPIE 4758, 9th International Conference on Ground Penetrating Radar,* S. Barbara, 2002.

[12] W. Al-Nuaimy, Y. Huang, M. T. C. Fang, V. T. Nguyen, A. Erikson, "Automatic detection of buried utilities and solid objects with GPR using neural networks and pattern recognition," *Journal of Applied Geophysics,* vol. 43, no. *2-4*, pp. *157-165*, 2000.

[13] F. Frezza, L. Pajewski, C. Ponti, G. Schettini, N. Tedeschi, "Cylindrical-Wave Approach for electromagnetic scattering by subsurface metallic targets in a lossy medium," *Journal of Applied Geophysics*, vol. *97*, pp. *55-59*, Oct., 2013.

[14] A. Giannopoulos, "Modelling ground penetrating radar by GprMax," *Construction Building Mater.*, vol. *19*, no. *10*, pp. *755–762*, Dec. 2005.

[15] Viola, P., Jones, M., "Rapid object detection using a boosted cascade of simple features," *In: Proc. IEEE Computer Society Conf. on Computer Vision and Pattern Recognition*, IEEE Computer Society, 2001, pp. *511-518*.

[16] C. Mass, J. Schmalzl, "Using pattern recognition to automatically localize reflection hyperbolas in data from ground penetrating radar", *Computers & Geosciences*, vol. *58*, pp. *116-125*, Aug., 2013.

[17] T. Ahonen, A. Hadid, M. Pietikainen, "Face Recognition with Local Binary Patterns", *in Proc. Computer vision - ECCV 2004, Lecture Notes in Computer Science*, vol. 3021, pp. 469–481.

[18] N. Dalal, B. Triggs, "Histograms of Oriented Gradients for Human Detection", *in Proc. IEEE Computer Society Conf. on Computer Vision and Pattern Recognition (CVPR '05)*, Jun 2005, San Diego, USA, pp. *886-893*.

[19] J. Canny, "A computational approach to edge detection", *IEEE Trans. Pattern Anal. Mach. Intell.*, vol. *8*, no *6*, pp. *679-698*, 1986.

[20] http://users.uoa.gr/~atzanis/matgpr/matgpr.html

[21] http://www.geophysical.com/softwareutilities.htm

[22] http://www.geophysical.com/software.htm